

The Effects of Nonzero Total Electron Spin in the \tilde{X}^3B_1 State of Methylene CH_2

Igor N. Kozin¹ and Per Jensen

FB 9—Theoretische Chemie, Bergische Universität—GH Wuppertal, D-42097 Wuppertal, Germany

Received January 28, 1997

We report here how we have incorporated the effects of a nonzero total electron spin in the MORBID Hamiltonian and computer program [P. Jensen, *J. Mol. Spectrosc.* **128**, 478–501 (1988); *J. Chem. Soc. Faraday Trans. 2* **84**, 1315–1340 (1988); in “Methods in Computational Molecular Physics” (S. Wilson and G. H. F. Diercksen, Eds.), Plenum Press, New York, 1992] for calculating the rovibronic energies of a triatomic molecule directly from the potential energy function. The spin–spin and spin–rotation Hamiltonian terms, given in a form depending on the vibrational coordinates, have been expressed in terms of isotope-independent functions and added to the MORBID rotation–vibration Hamiltonian. The eigenvalues of the resulting Hamiltonian are obtained in a variational procedure. This method is tested on the methylene radical CH_2 in the \tilde{X}^3B_1 electronic ground state for which we describe simultaneously the splittings due to electron spin for the isotopomers $^{12}\text{CH}_2$, $^{12}\text{CD}_2$, and $^{13}\text{CH}_2$. For these molecules, experimental data are available, and we compare the results of least-squares fits to these data with predictions from *ab initio* theory. © 1997

Academic Press

I. INTRODUCTION

The present paper is concerned with the calculation of the rovibronic energies of triatomic molecules in isolated, nonsinglet electronic states. We give a detailed description of how we incorporate the effects of a nonvanishing electron spin into a variational calculation of these energies. Our work is based on the MORBID (Morse Oscillator Rigid Bender Internal Dynamics) Hamiltonian and computer program (1–3) for the variational calculation of the rotation–vibration energy levels in an isolated singlet electronic state of a triatomic molecule from the potential energy function.

A “classical” model, developed for the purpose of fitting to observed molecular spectra, is based on an effective Hamiltonian. This Hamiltonian contains effective parameters whose values in most cases can only be determined by fitting to experimental data. In principle, these values could also be obtained by means of perturbation theory from underlying parameters defining more fundamental physical properties of the molecule, such as the Born–Oppenheimer potential function or the dipole moment function. However, in many instances the relation between the two sets of parameters is not known in practice, and so the interpretation of the spectra of a molecule does not provide knowledge about its fundamental properties. Alternatively, for small molecules it is possible to calculate observable quantities directly from the

functions defining the fundamental properties. Specifically, the rovibronic energies can be calculated directly from the potential energy surface (1–7), and the potential energy function can be refined by fitting to experimentally derived term values or experimental transition frequencies (see, for example, Refs. (3, 8), and the references cited in them). One obvious advantage of this type of approach is that within the Born–Oppenheimer approximation, the potential energy surface is isotope independent, so that data for all isotopomers can often be fitted simultaneously. However, to our knowledge methods for the direct calculation of rovibronic energies from the potential energy surface in an isolated electronic state have so far only been available for singlet states, i.e., states with zero electron spin. In the present work, we report an extension of the MORBID Hamiltonian and computer program (1–3) to account also for the spin–rotation and spin–spin interaction caused by a nonvanishing electron spin. The factors in the spin–rotation and spin–spin Hamiltonian terms, which depend on the vibrational coordinates, are expressed in terms of isotope-independent functions. By analogy with the calculation of rotation–vibration energies from the potential function, our approach enables the electron spin effects in different isotopomers to be described using a common set of parameters.

We have applied the extended program to the \tilde{X}^3B_1 electronic ground state of the methylene radical CH_2 . Methylene is the prototype carbene and an intermediate in many chemical reactions; this makes it an important molecule to study. In addition, CH_2 is of astrophysical interest. It has recently been identified in interstellar space by Hollis *et al.* (9), after a tentative identification had been reported by the same

¹ On leave from Applied Physics Institute, Russian Academy of Science, Uljanov Street 47, Nizhnii Novgorod, 603600, Russia. Present address: Université du Littoral, Boîte postale 5526, F-59379 Dunkerque Cedex 1, France.

authors some years ago (10). Very recent laboratory investigations of the rotational spectrum (11, 12) are aimed at facilitating further observations in the interstellar medium.

An important consideration in our choice of \tilde{X}^3B_1 CH₂ for the application of our new program is the fact that there is a considerable amount of experimental information available (11–21) (see also Ref. (22)), in which the spin splittings are resolved. This means that we have input data for fitting to experiment. Another important consideration is that there exist *ab initio* calculations of the electron spin effects (23–27) with which we can compare the results of our least-squares fits.

II. THE HAMILTONIAN

Reference (1) gives a complete account of the MORBID Hamiltonian \hat{H}_{vr} which describes the rotation and vibration of a triatomic molecule in an isolated singlet electronic state. It is well known that in order to treat the effects of a nonvanishing electron spin, we must add to \hat{H}_{vr} two terms, \hat{H}_{sr} and \hat{H}_{ss} , which describe spin–rotation interaction and spin–spin interaction, respectively. Hence, in the present work we employ the following Hamiltonian:

$$\hat{H} = \hat{H}_{\text{vr}} + \hat{H}_{\text{sr}} + \hat{H}_{\text{ss}}. \quad [1]$$

Following van Vleck (28) and Raynes (29), we express \hat{H}_{sr} and \hat{H}_{ss} as

$$\hat{H}_{\text{sr}} = \sum_{\beta\gamma} \epsilon_{\beta\gamma}(\bar{\rho}, \Delta r_{12}, \Delta r_{32}) \hat{N}_{\beta} \hat{S}_{\gamma}, \quad [2]$$

and

$$\hat{H}_{\text{ss}} = \sum_{\beta\gamma} \alpha_{\beta\gamma}(\bar{\rho}, \Delta r_{12}, \Delta r_{32}) \hat{S}_{\beta} \hat{S}_{\gamma}, \quad [3]$$

respectively, where β and γ assume the values x, y , and z , and \hat{S}_{β} and \hat{N}_{β} are the components along the molecule-fixed β -axis of the electron spin \mathbf{S} and the total angular momentum less the electron spin

$$\mathbf{N} = \mathbf{J} - \mathbf{S}, \quad [4]$$

respectively. In a standard, effective-Hamiltonian treatment of the spin–rotation and spin–spin interactions, the quantities $\epsilon_{\beta\gamma}$ and $\alpha_{\beta\gamma}$ in Eqs. [2] and [3] would be assumed to be effective parameters, depending on the vibrational state under study. In the present work we take them to be functions of the vibrational coordinates ($\bar{\rho}, \Delta r_{12}, \Delta r_{32}$) used in the MORBID approach. The angle $\bar{\rho}$ is the instantaneous value of the supplement of the bond angle (see Ref. (1) and the references cited in it), and $\Delta r_{j2} = r_{j2} - r_{j2}^e$, where r_{j2} is the instantaneous distance between the “terminal” nucleus j (=

1 or 3) and the “central” nucleus 2, and r_{j2}^e is the equilibrium value of r_{j2} .

We choose the molecule-fixed axis system xyz as described in Ref. (1) (in particular, see Fig. 1 of Ref. (1)). It is a right-handed axis system, and the three nuclei of the molecule define the yz plane. The location of the xyz axis system relative to the instantaneous locations of the nuclei is defined by the center-of-mass, Eckart and Sayvetz conditions given in Eqs. [9]–[11] of Ref. (1).

It is well known that in the standard, effective-Hamiltonian treatment, a diagonal ϵ -parameter $\epsilon_{\beta\beta}$ is, in a first approximation, inversely proportional to the moment of inertia $I_{\beta\beta}$ associated with the β axis (see Ref. (29)). This has been confirmed for many molecules by relations such as

$$\frac{\epsilon'_{aa}}{\epsilon_{aa}} = \frac{A'}{A}, \quad [5]$$

where ϵ'_{aa} and ϵ_{aa} are ϵ -parameters for two different isotopomers of a molecule, and A' and A are the corresponding A rotational constants, which are approximately proportional to I_{aa}^{-1} . By using relations such as that in Eq. [5], it would obviously be possible to parameterize \hat{H}_{sr} in terms of isotope-independent parameters. In the present work, we obtain such a parameterization by modeling $\epsilon_{\beta\gamma}$ in the following way:

$$\begin{aligned} \epsilon_{\beta\gamma}(\bar{\rho}, \Delta r_{12}, \Delta r_{32}) \\ = \sum_{\delta} \mu_{\beta\delta}(\bar{\rho}, \Delta r_{12}, \Delta r_{32}) f_{\delta\gamma}(\bar{\rho}, \Delta r_{12}, \Delta r_{32}). \end{aligned} \quad [6]$$

In Eq. [6], $\mu_{\beta\delta}$ is an element of the inverse inertial tensor $\boldsymbol{\mu} = (\mathbf{I}')^{-1}$, where the elements of the tensor \mathbf{I}' are given by Eqs. [16] and [17] of Ref. (1). We assume that the functions $f_{\delta\gamma}(\bar{\rho}, \Delta r_{12}, \Delta r_{32})$ of Eq. [6] are isotope independent.

We cannot rigorously derive the expression for the functions $\epsilon_{\beta\gamma}(\rho, \Delta r_{12}, \Delta r_{32})$ in Eq. [6], but we can make it plausible by following the arguments given by Raynes (29) in his first-approximation treatment of spin–rotation interaction. Raynes (29) gives the Hamiltonian function for the spin–rotation interaction as

$$H_{\text{sr}} = - \frac{g_e \mu_B}{4\pi \epsilon_0 c^2} \sum_n \sum_j \left[\frac{Z_n e}{r_{jn}^3} \right] [(\mathbf{r}_j - \mathbf{r}_n) \times \mathbf{v}_n] \cdot \mathbf{S}_j, \quad [7]$$

where the instantaneous position and velocity vectors of nucleus n are denoted \mathbf{r}_n and \mathbf{v}_n , respectively, while the position vector and spin angular momentum of electron j are denoted \mathbf{r}_j and \mathbf{S}_j , respectively. The quantity r_{jn} is the distance between nucleus n and electron j , Z_n is the atomic number of nucleus n , $g_e = 2\mu_e/\mu_B$ is the electronic g factor (30), μ_B is the Bohr magneton, ϵ_0 is the permittivity of vacuum, c is

the velocity of light in vacuum, and e is the elementary charge. We have “translated” the original expression by Raynes into SI units of energy (31). When we follow Raynes (29) in approximating the nuclear velocity \mathbf{v}_n by

$$\mathbf{v}_n \approx \boldsymbol{\omega} \times \mathbf{r}_n \quad [8]$$

with the angular velocity $\boldsymbol{\omega}$ approximated by

$$\boldsymbol{\omega} \approx \boldsymbol{\mu} \mathbf{N}, \quad [9]$$

we obtain the expression for \hat{H}_{sr} given by Eqs. [2] and [6] with $f_{\delta\gamma}$ functions given by

$$f_{\gamma\gamma} = -\frac{g_e \mu_B}{4\pi \epsilon_0 c^2} \left\langle \psi_e \left| \sum_{nj} \frac{Z_n e}{r_{jn}^3} [r_{\nu n}(r_{\nu j} - r_{\nu n}) + r_{\eta n}(r_{\eta j} - r_{\eta n})] \kappa_j(\gamma) \right| \psi_e \right\rangle_{\text{el}} \quad [10]$$

and

$$f_{\gamma\nu} = \frac{g_e \mu_B}{4\pi \epsilon_0 c^2} \left\langle \psi_e \left| \sum_{nj} \frac{Z_n e}{r_{jn}^3} (r_{\gamma j} - r_{\gamma n}) r_{\nu n} \kappa_j(\gamma) \right| \psi_e \right\rangle_{\text{el}}. \quad [11]$$

In Eqs. [10] and [11], $\gamma\nu\eta$ is a cyclic permutation of xyz , $r_{\nu n}$ and $r_{\nu j}$ are the ν -components ($\nu = x, y, z$) of the vectors \mathbf{r}_n and \mathbf{r}_j , respectively, $\kappa_j(\gamma)$ is a constant factor arising from the linear dependence of $s_{\gamma j}$, the γ -component of \mathbf{s}_j ($\gamma = x, y, z$), on S_γ , the γ -component of the total electron spin \mathbf{S} . Finally, ψ_e is the electronic wavefunction of the electronic state under study and the subscript “el” on the expectation value indicates that integration is to be performed over the electronic coordinates only, so that the functions $f_{\delta\gamma}$ will depend on the nuclear coordinates. Our $f_{\gamma\nu}$ factors correlate with Raynes’ $a_{\gamma\nu}$ parameters given in the appendix of Ref. (29).

Since we consider only triatomic, planar molecules, Eq. [6] can be simplified somewhat. The nonvanishing $\epsilon_{\beta\gamma}$, $\mu_{\beta\gamma}$, and $f_{\beta\gamma}$ components are related as

$$\begin{aligned} \epsilon_{xx} &= \mu_{xx} f_{xx}, \\ \epsilon_{yy} &= \mu_{yy} f_{yy} + \mu_{yz} f_{zy}, \\ \epsilon_{yz} &= \mu_{yy} f_{yz} + \mu_{yz} f_{zy}, \\ \epsilon_{zy} &= \mu_{yz} f_{yy} + \mu_{zz} f_{zy}, \\ \epsilon_{zz} &= \mu_{yz} f_{yz} + \mu_{zz} f_{zz}, \end{aligned} \quad [12]$$

where we have not explicitly indicated that all of these functions depend on $(\bar{\rho}, \Delta r_{12}, \Delta r_{32})$.

By analogy with the expansion for the potential energy

function used in the MORBID approach (1–3), we expand the $f_{\beta\gamma}$ functions to second order in Δr_{12} and Δr_{32} :

$$f_{\beta\gamma} = (f_{\beta\gamma}) + (f_{\beta\gamma})_1 \Delta r_{12} + (f_{\beta\gamma})_3 \Delta r_{32} + (f_{\beta\gamma})_{11} \Delta r_{12}^2 + (f_{\beta\gamma})_{33} \Delta r_{32}^2 + (f_{\beta\gamma})_{13} \Delta r_{12} \Delta r_{32}. \quad [13]$$

The expansion coefficients $(f_{\beta\gamma})_i \dots$ depend on the bending coordinate as

$$(f_{\beta\gamma})_{i\dots} = (f_{\beta\gamma})_{i\dots}^{(0)} + (f_{\beta\gamma})_{i\dots}^{(1)} (\cos \rho_e - \cos \bar{\rho}) + (f_{\beta\gamma})_{i\dots}^{(2)} (\cos \rho_e - \cos \bar{\rho})^2. \quad [14]$$

There is one slight technical difficulty here. We parameterize the $f_{\beta\gamma}$ functions to depend on $\bar{\rho}$, the instantaneous value of the supplement of the bond angle, exactly as it is done for the potential energy function in the MORBID approach (1). In order that they can be used in the calculations, the $f_{\beta\gamma}$ functions must be transformed to depend on the “true” bending coordinate ρ . This is done as described for the potential energy function in Ref. (1). When the molecule is symmetrical, i.e., of type ABA, the number of independent parameters in the expansions for the $f_{\beta\gamma}$ functions is reduced by symmetry. For example, $(f_{xx})_1^{(0)} = (f_{xx})_3^{(0)}$. We expand the spin–spin interaction functions (Eq. [3]) in a manner analogous to the $f_{\beta\gamma}$ expansions,

$$\begin{aligned} \alpha_{\beta\gamma} &= (\alpha_{\beta\gamma}) + (\alpha_{\beta\gamma})_1 \Delta r_{12} + (\alpha_{\beta\gamma})_3 \Delta r_{32} \\ &+ (\alpha_{\beta\gamma})_{11} \Delta r_{12}^2 + (\alpha_{\beta\gamma})_{33} \Delta r_{32}^2 \\ &+ (\alpha_{\beta\gamma})_{13} \Delta r_{12} \Delta r_{32}, \end{aligned} \quad [15]$$

where $(\alpha_{\beta\gamma})_{i\dots}$ is expanded as in Eq. [14].

Special care must be taken to ensure that the $f_{\beta\gamma}$ functions, and hence the $\epsilon_{\beta\gamma}$ functions, behave correctly when the molecule becomes linear, i.e., when $\bar{\rho} = 0$. Because of the higher symmetry ($C_{\infty v}$ or $D_{\infty h}$) of this configuration, we can impose useful constraints on the $f_{\beta\gamma}$ and $\alpha_{\beta\gamma}$ functions. When $\bar{\rho} = 0^\circ$ and the molecule is linear along the z axis, $\epsilon_{yy} - \epsilon_{xx} = 0$ and $\alpha_{yy} - \alpha_{xx} = 0$. In this configuration, $\mu_{yy} = \mu_{xx}$ and $\mu_{yz} = 0$, and consequently $f_{yy} - f_{xx} \rightarrow 0$ for $\bar{\rho} \rightarrow 0$. In principle, we could introduce similar constraints for the situation with $\bar{\rho} = 180^\circ$, when the molecule is linear along the y axis, but as the potential energy function attains extremely large values at such configurations, these constraints would have little practical importance and so we have used them only for test purposes. Finally, we have chosen in practice to parameterize the following set of functions: $(f_{yy} - f_{xx})$, $(f_{yy} + f_{xx})$, f_{zz} , f_{yz} , f_{zy} , $(\alpha_{yy} - \alpha_{xx})$, $(\alpha_{zz} - \alpha_{xx})$, $(\alpha_{xx} + \alpha_{yy} + \alpha_{zz})$, and α_{yz} . They were all expanded as indicated by Eqs. [13] and [14] with the exception that we have forced $(f_{yy} - f_{xx})$ and $(\alpha_{yy} - \alpha_{xx})$ to go to zero for $\bar{\rho} \rightarrow 0$ by multiplying the expansions given by Eqs. [13] and [14] by $(1 - \cos \bar{\rho})/(1 - \cos \rho_e)$

(so that the equilibrium value of the function in question does not change). Obviously, this latter step is not necessary for a linear molecule with $\rho_e = 0$, since for such a molecule we can simply set all $(\alpha_{yy} - \alpha_{xx})_{i..}^{(0)}$ and $(f_{yy} - f_{xx})_{i..}^{(0)}$ equal to zero.

In setting up the matrix representations of \hat{H}_{sr} and \hat{H}_{ss} , we use the techniques described by Brown and Howard (32) and by Bowater *et al.* (33), with some slight modification owing to the fact that the phase choice of the rotational functions used in the MORBID approach differs from the more standard choice made in Refs. (32, 33) (see Eq. [50] of Ref. (34)). We use decoupled space-fixed rotation–spin basis functions which are given by

$$|NJSkM_J\rangle = \sum_{M=-N}^N \sum_{M_S=-S}^S (-1)^{N-S+M_J} \sqrt{2J+1} \times \begin{pmatrix} N & S & J \\ M & M_S & -M_J \end{pmatrix} |SM_S\rangle |NkM\rangle. \quad [16]$$

This function is a simultaneous eigenfunction for \hat{N}^2 [with eigenvalue $\hbar^2 N(N+1)$], \hat{J}^2 [with eigenvalue $\hbar^2 J(J+1)$], \hat{S}^2 [with eigenvalue $\hbar^2 S(S+1)$], \hat{N}_z [with eigenvalue $\hbar k$], and \hat{J}_z , the component of \mathbf{J} along the space-fixed quantization axis Z [with eigenvalue $\hbar M_J$]. In Eq. [16], the quantity in parentheses is a $3j$ symbol (35), $|SM_S\rangle$ is an electron spin function quantized along space fixed axes, and $|NkM\rangle$ is an eigenfunction for the rigid symmetric rotor (36).

To evaluate effectively the matrix elements of \hat{H}_{ss} and \hat{H}_{rs} it is advantageous to express these operators in terms of irreducible tensor operators $T_q^{(\sigma)}$ (35). From the nonvanishing tensor elements $\epsilon_{\beta\gamma}$ and $\alpha_{\beta\gamma}$, we can form the following irreducible tensor operators:

$$\begin{aligned} T_0^{(1)}(\mathbf{N}) &= \hat{N}_z & T_0^{(1)}(\mathbf{S}) &= \hat{S}_z \\ T_{\pm 1}^{(1)}(\mathbf{N}) &= \frac{1}{\sqrt{2}} (\mp \hat{N}_x - i\hat{N}_y) & T_{\pm 1}^{(1)}(\mathbf{S}) &= \frac{1}{\sqrt{2}} (\mp \hat{S}_x - i\hat{S}_y) \\ T_0^{(0)}(\epsilon) &= -\frac{1}{\sqrt{3}} (\epsilon_{xx} + \epsilon_{yy} + \epsilon_{zz}) \\ T_0^{(0)}(\alpha) &= -\frac{1}{\sqrt{3}} (\alpha_{xx} + \alpha_{yy} + \alpha_{zz}) \\ T_{\pm 1}^{(1)}(\epsilon) &= \pm \frac{i}{2} (\epsilon_{yz} - \epsilon_{zy}) \\ T_0^{(2)}(\epsilon) &= \frac{1}{\sqrt{6}} (2\epsilon_{zz} - \epsilon_{xx} - \epsilon_{yy}) \\ T_0^{(2)}(\alpha) &= \frac{1}{\sqrt{6}} (2\alpha_{zz} - \alpha_{xx} - \alpha_{yy}) \\ T_{\pm 1}^{(2)}(\epsilon) &= -\frac{i}{2} (\epsilon_{yz} + \epsilon_{zy}) & T_{\pm 1}^{(2)}(\alpha) &= -i\alpha_{yz} \\ T_{\pm 2}^{(2)}(\epsilon) &= \frac{1}{2} (\epsilon_{xx} - \epsilon_{yy}) & T_{\pm 2}^{(2)}(\alpha) &= \frac{1}{2} (\alpha_{xx} - \alpha_{yy}). \end{aligned}$$

In terms of these operators, the Hamiltonian for spin–rotation interaction takes the form

$$\hat{H}_{sr} = \frac{1}{2} \sum_{\sigma=0}^2 [T^{(\sigma)}(\epsilon) \cdot T^{(\sigma)}(\mathbf{N}, \mathbf{S}) + T^{(\sigma)}(\mathbf{N}, \mathbf{S}) \cdot T^{(\sigma)}(\epsilon)], \quad [17]$$

where the generalized dot product of two irreducible tensor operators is given by Eq. (5.47) of Ref. (35), e.g.,

$$T^{(\sigma)}(\epsilon) \cdot T^{(\sigma)}(\mathbf{N}, \mathbf{S}) = \sum_{p=-\sigma}^{\sigma} (-1)^q T_p^{(\sigma)}(\epsilon) T_{-p}^{(\sigma)}(\mathbf{N}, \mathbf{S}) \quad [18]$$

and

$$T_p^{(\sigma)}(\mathbf{N}, \mathbf{S}) = (-1)^p \sqrt{2\sigma+1} \times \sum_{p_1 p_2} T_{p_1}^{(1)}(\mathbf{N}) T_{p_2}^{(1)}(\mathbf{S}) \begin{pmatrix} 1 & 1 & \sigma \\ p_1 & p_2 & -p \end{pmatrix}. \quad [19]$$

The matrix elements of \hat{H}_{sr} are

$$\begin{aligned} \langle N' J' S' k' M'_J | \hat{H}_{sr} | N J S k M_J \rangle &= \frac{1}{2} \delta_{J'J} \delta_{M'_J M_J} \delta_{S'S} \sqrt{(2S+1)S(S+1)} \\ &\times \sqrt{(2N'+1)(2N+1)} \times (-1)^{J-k'+S} \\ &\times \begin{Bmatrix} N & S & J \\ S & N' & 1 \end{Bmatrix} \sum_{\sigma=0}^2 \sqrt{2\sigma+1} \\ &\times \left[(-1)^{\sigma} \sqrt{(2N+1)N(N+1)} \begin{Bmatrix} 1 & 1 & \sigma \\ N' & N & N \end{Bmatrix} \right. \\ &\left. + \sqrt{(2N'+1)N'(N'+1)} \begin{Bmatrix} 1 & 1 & \sigma \\ N & N' & N' \end{Bmatrix} \right] \\ &\sum_q i^{k-k'} T_q^{(\sigma)}(\epsilon) \begin{pmatrix} N' & \sigma & N \\ -k' & q & k \end{pmatrix}. \end{aligned} \quad [20]$$

Apart from a factor $i^{k-k'}$ originating in the fact that our phase choice for the basis functions is different from that of Bowater *et al.* (33), this is the result given in their Eq. (30). Because of the factor $i^{k-k'}$, all terms in Eq. [20] are real. With definitions analogous to Eqs. [18] and [19], we have for the spin–spin interaction Hamiltonian

$$\hat{H}_{ss} = \sum_{\sigma=0}^2 T^{(\sigma)}(\alpha) \cdot T^{(\sigma)}(\mathbf{S}, \mathbf{S}). \quad [21]$$

Its matrix elements are

$$\begin{aligned}
 \langle N'J'S'k'M_J' | \hat{H}_{ss} | NJSkM_J \rangle \\
 = \delta_{J'J} \delta_{M_J'M_J} \delta_{S'S} (2S+1)S(S+1) \\
 \times \sqrt{(2N'+1)(2N+1)} (-1)^{N'+N+J-k'-S} \\
 \times \sum_{\sigma=0}^2 \sqrt{2\sigma+1} \begin{Bmatrix} S & \sigma & S \\ 1 & S & 1 \end{Bmatrix} \begin{Bmatrix} S & N & J \\ N' & S & \sigma \end{Bmatrix} (-1)^\sigma \\
 \times \sum_q i^{k-k'} T_q^{(\sigma)}(\alpha) \begin{pmatrix} N' & \sigma & N \\ -k' & q & k \end{pmatrix},
 \end{aligned} \quad [22]$$

where again the factor $i^{k-k'}$ appears because of our phase choice for the basis functions.

The symmetrized spin-rotation basis functions are given by

$$|NJSKM_J\tau\rangle = \frac{1}{\sqrt{2}} [|NJSKM_J\rangle + (-1)^{N+K+\tau} |NJS-KM_J\rangle], \quad [23]$$

where $K > 0$ and the integer τ assumes the values 0 or 1. For $K = 0$,

$$|NJS0M_J\tau\rangle = |NJS0M_J\rangle \quad [24]$$

and $\tau = N \bmod 2$. The total spin-rotation-vibration basis functions, used to construct the matrix representation of the total Hamiltonian \hat{H} of Eq. [1], are obtained by multiplying the $|NJSKM_J\tau\rangle$ of Eq. [23] by the vibrational basis functions described in Ref. (1). It follows from Eqs. [20] and [22] that the Hamiltonian matrix is diagonal in J , M_J , and S . We have extended the MORBID computer program (1-3), so that it constructs the matrix representation of \hat{H} in the basis described above and diagonalizes it by means of standard numerical methods.

III. APPLICATION TO METHYLENE

As mentioned in Section I, we have applied the new computer program to the methylene radical CH_2 in its \tilde{X}^3B_1 ground electronic state. High resolution spectra of $\tilde{X}^3B_1 \text{CH}_2$ in the gas phase were studied intensively a decade ago, in particular by means of laser magnetic resonance (LMR) (13), diode laser absorption spectroscopy (16), and microwave spectroscopy (18). The spectra are known for $^{12}\text{CH}_2$ in the vibrational states $(v_1v_2v_3) = (000)$, (010) (17), and (100) (19), for $^{12}\text{CD}_2$ in the vibrational states (000), (010), and (100) (20), and for $^{13}\text{CH}_2$ in the vibrational states (000) and (010) (21). Very recently, submillimeter-wave investigations of CH_2 (11) and CD_2 (12) have been reported. In all the experimental work mentioned here, the splittings re-

sulting from spin-rotation and spin-spin interaction were resolved, and so we have an extensive data set which we can use to test the validity of our model for the spin effects.

In principle, it would be possible to obtain spin-rotation and spin-spin interaction parameters by fitting directly to experimentally observed wavenumbers and frequencies. However, this is not an efficient procedure. The reason is that we can calculate accurate spin splittings with a much smaller vibrational basis set than we need to calculate accurately the experimentally observed rovibronic energy differences. Another problem with CH_2 is that since most of the experimental data were obtained in laser magnetic resonance experiments, the published wavenumbers were obtained at nonzero magnetic fields, so that zero-field values would have to be obtained by extrapolation. In view of these facts, we decided to use the effective spin-rotation and spin-spin interaction parameters reported in the publications cited above to calculate spin splittings and then to use these as input data for our fitting. For this purpose, we used a very powerful program, which is made available to the spectroscopic community by H. M. Pickett (37). We included in the input data for the fitting only splittings for levels involved in observed transitions. Because $\tilde{X}^3B_1 \text{CH}_2$ is quasilinear (it has a barrier to linearity of less than 2000 cm^{-1}) the spin splittings depend strongly on K_a , whereas the dependence on N is much less drastic. Hence, we used only spin splittings for $N \leq (K_a)_{\max}$ in the input data, where $(K_a)_{\max}$ is the maximum K_a value, for which transitions have been observed for the vibrational state in question. The input data set contained 125 entries in total. For $^{12}\text{CH}_2$, there were 70 data points belonging to the vibrational states $(v_1v_2v_3) = (000)$ ($(K_a)_{\max} = 4$), (010) ($(K_a)_{\max} = 2$), and (100) ($(K_a)_{\max} = 1$). For $^{12}\text{CD}_2$, there were 33 data points for the states (000) ($(K_a)_{\max} = 2$), (010) ($(K_a)_{\max} = 2$), and (100) ($(K_a)_{\max} = 2$), and finally for $^{13}\text{CH}_2$, there were 22 data points for the states (000) ($(K_a)_{\max} = 2$) and (010) ($(K_a)_{\max} = 1$). The spin splittings to be used as input data for the fitting were generated from the effective parameters given in Refs. (13-21). We did not use the parameters from Refs. (11, 12), obtained in submillimeter-wave experiments, to calculate input data. The reason is that these experiments yielded only very few transitions, and in the analysis almost all parameters were constrained to values from Refs. (13-21). Hence we suspect that splittings calculated from the submillimeter parameters may not be consistent with those calculated from the parameters of Refs. (13-21), which were obtained from a much larger, statistically more significant experimental data set.

We could fit the 125 data points by usefully varying eight parameters, whose optimized values we report in Table 1. All fitted data points were given equal weights. The potential parameters were kept at the values reported in Ref. (38). To obtain well converged spin splittings, a rather small vibrational basis was sufficient: from six to four bending functions

TABLE 1
Fitted Spin Interaction Parameters for Methylene

$(f_{yy} + f_{xx})^{(0)} \times 10^3$	-0.5899(74) ^a	$(\alpha_{zz} - \alpha_{xx})^{(0)}/\text{cm}^{-1}$	0.8085(16)
$(f_{zz})^{(0)} \times 10^5$	-0.492(91)	$(\alpha_{zz} - \alpha_{xx})^{(1)}/\text{cm}^{-1}$	-0.054(15)
$(\alpha_{yy} - \alpha_{xx})^{(0)}/\text{cm}^{-1}$	0.08340(94)	$(\alpha_{zz} - \alpha_{xx})^{(2)}/\text{cm}^{-1}$	0.323(34)
$(\alpha_{yy} - \alpha_{xx})^{(1)}/\text{cm}^{-1}$	-0.041(11)	$(\alpha_{zz} - \alpha_{xx})_1^{(0)}/\text{cm}^{-1}$	0.184(43)

^aQuantities in parentheses are standard errors in units of the last digit given.

and six stretching functions. Consequently, one iteration of the nonlinear least squares fitting procedure required only 100 min of CPU time on an IBM RISC/6000 3AT workstation with 192 MB RAM. We were only able to fit one parameter describing the dependence of the modeled functions on the stretching coordinates, the parameter $(\alpha_{zz} - \alpha_{xx})_1^{(0)}$. This is not so surprising since only very few data points are available for excited stretching states. The total standard deviation of the fitting was 0.0015 cm^{-1} , with a slightly better root-mean-square deviation obtained for the CD₂ data taken alone. A further decrease in the standard deviation could perhaps be obtained by introducing a more sophisticated weighting scheme rather than the equal weights used. This, however, would require detailed knowledge of the uncertainties of the spin splittings obtained in the different experiments.

IV. DISCUSSION

It is not straightforward to compare the results of the present work directly to the effective spin-rotation and spin-spin interaction parameters obtained from analyses of experimental data. One way would be to compare the calculated spin splittings to the corresponding experimental values, but we do not consider it feasible to publish the resulting extensive tables of spin splittings. To provide a “compact” comparison with experiment, we have sought to use our theory for predicting the leading parameters in the commonly used effective Hamiltonian treatment of electron spin effects (14, 39)

$$\hat{H}_{\text{eff}} = \sum_{\nu\eta} \epsilon_{\nu\eta} N_{\nu} S_{\eta} + D(S_a^2 - S^2/3) + E(S_b^2 - S_c^2), \quad [25]$$

where ν and η run over the principal axis labels a , b , and c (which correspond to the z , y , and x axes, respectively, in our treatment of CH₂). We assume that in a first approximation, the values of the effective parameters can be given by vibrational expectation values of the largest $\epsilon_{\beta\gamma}$ and $\alpha_{\beta\gamma}$ tensor elements which, in our theoretical treatment, also have matrix elements off-diagonal in the vibrational wavefunctions. It is useful to note that for the conventional I^r molecule-fixed axis choice there is a simple correlation between

our spin-spin parameters and the widely used D and E parameters:

$$D = (\alpha_{zz} - \alpha_{xx}) - (\alpha_{yy} - \alpha_{xx})/2;$$

$$(\alpha_{zz} - \alpha_{xx}) = D + E; \quad [26]$$

$$E = (\alpha_{yy} - \alpha_{xx})/2; \quad (\alpha_{yy} - \alpha_{xx}) = 2E. \quad [27]$$

We report in Table 2 calculated estimates of spin-rotation and spin-spin interaction parameters for the ground vibrational states of ¹²CH₂, ¹²CD₂, and ¹²CHD. In the same table the experimental parameters for the ground vibrational states of ¹²CH₂ and ¹²CD₂ are also given for reference purposes. There is generally a good agreement between calculation and experiment. The experimental values are often “averaged” over the observed range of K_a values. For instance, in the analyses of the experimental data the ϵ_{aa} parameters were not considered to depend on K_a . In the MORBID approach however, the bending wavefunctions depend on K_a , and so the vibrationally averaged values of $\epsilon_{\beta\gamma}$ and $\alpha_{\beta\gamma}$ will also depend on K_a . The calculated values in Table 2 are obtained for $K_a = 0$. In view of this, it is not surprising that the calculated $K_a = 0$ value for ϵ_{aa} deviates most from the experimental value, since this parameter depends strongly on K_a (see below). It is found that the largest calculated value of ϵ_{aa} is obtained for $K_a = 0$, but this value does not influence the spin splittings observed for $K_a = 0$ (since in this case, it is multiplied by a zero matrix element of \hat{N}_z) and so in the analysis of the experiment, this value drops out of the “averaging.”

In the effective-Hamiltonian treatment of high K_a states of methylene, a so-called D_{SK} term has been added to the effective Hamiltonian to describe the dependence of D on K_a (17). With this term, the second term on the right-hand side of Eq. [25] is modified to be $(D + D_{SK}K_a^2)(S_a^2 - S^2/3)$. This implies that the dependence of D on K_a should be quadratic. It is evident from Figs. 1 and 2 that even for the vibrational ground state, neither D nor E depends quadratically on K_a . This dependence is more likely to be linear. For some of the excited bending states the change in D with K_a would seem to suggest a correction inversely proportional to K_a . Thus caution must be taken when using predictions of D 's for higher K_a value. Nevertheless, to compare with experiment, we have fitted the function $D + D_{SK}K_a^2$ through the values of D calculated for K_a from 0 to 4 in the vibrational ground state of ¹²CH₂, thus obtaining the values of D and D_{SK} given in Table 2.

Table 3 summarizes the calculated spin-spin and spin-rotation interaction parameters for the six lowest vibrational states of ¹²CH₂. It is seen that the parameters change significantly upon excitation of the bending mode, whereas excitation of the stretching modes causes much smaller changes. It is especially obvious for ϵ_{aa} , but perhaps the prediction of

TABLE 2

Comparison of Experimental and Calculated Spin Interaction Parameters (in cm^{-1}) for the Ground Vibrational States of $^{12}\text{CH}_2$, ^{12}CHD , and $^{12}\text{CD}_2$

	$^{12}\text{CH}_2$		^{12}CHD	$^{12}\text{CD}_2$	
	experiment ^a	calculated	calculated	experiment ^b	calculated
$\epsilon_{aa} \times 10^2$	0.048	0.096	0.063	0.028	0.040
$\epsilon_{bb} \times 10^2$	-0.512	-0.499	-0.335	-0.260	-0.250
$\epsilon_{cc} \times 10^2$	-0.412	-0.430	-0.294	-0.208	-0.220
$\epsilon_{ba} \times 10^2$	0.	-0.002	0.008	0.	0.
$\epsilon_{ab} \times 10^2$	0.	0.010	-0.046	0.	0.003
D	0.7788	0.7773 ^c	0.7797	0.7765	0.7753
$D_{SK} \times 10^3$	-0.832	-0.780 ^c			
$E \times 10$	0.4059	0.4033	0.4055	0.4058	0.4064

^aExperimental parameters were taken from Ref. (17).
^bExperimental parameters were taken from Ref. (20).
^cThese two parameters were obtained by fitting the calculated D values for K_a from 0 to 4. See the text for further details.

this parameter is of limited interest for the reasons mentioned above. The variation of the most important parameters with K_a is given graphically in Figs. 1–3.

The electron spin effects in methylene have been the subject of several *ab initio* studies (23–27), and it is interesting to compare these purely theoretical results with those from the fittings of the present work. Obviously the most important feature of the electronic integrals describing spin–rotation and spin–spin interaction is their dependence on the bending angle. In Fig. 4, we show the parameter $\alpha_{zz} - \alpha_{xx} = D + E$ as a function of $\bar{\rho}$, and Fig. 5 is an analogous diagram for $\alpha_{yy} - \alpha_{xx} = 2E$. The solid curves represent the functions obtained

from Eq. [14] with the parameter values from Table 1. The dashed curves represent smooth interpolations between the *ab initio* points calculated by Langhoff and Davidson (25). These calculations do not include the spin–orbit contribution which is estimated to be relatively small. It is seen that for low and moderate values of $\bar{\rho}$, there is good agreement between the *ab initio* results and those obtained in the present work, whereas there are significant deviations for high $\bar{\rho}$ values. However, this is to be expected since our experimental input data only contain information about states with $v_2 \leq 1$, and hence we can only probe the geometry-dependent functions in a $\bar{\rho}$ interval close to the equilibrium value of $\bar{\rho}$, $\rho_e = 46.0692^\circ$.

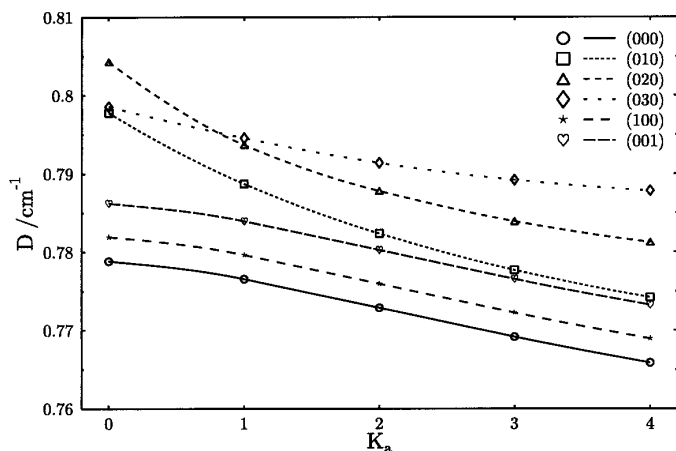


FIG. 1. Calculated values of D for K_a ranging from 0 to 4 for the lowest vibrational states of $^{12}\text{CH}_2$.

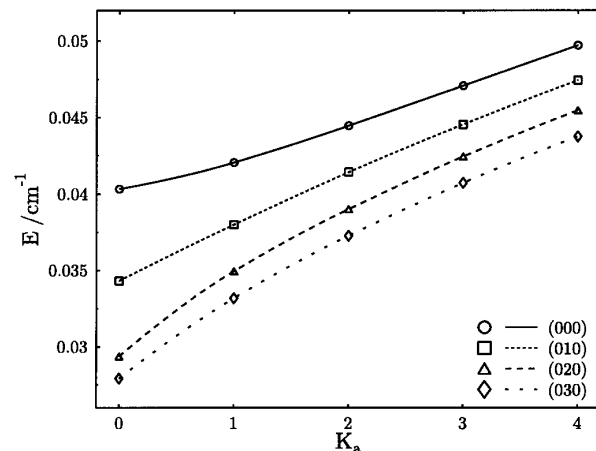


FIG. 2. Calculated values of E for K_a ranging from 0 to 4 for the lowest vibrational states of $^{12}\text{CH}_2$.

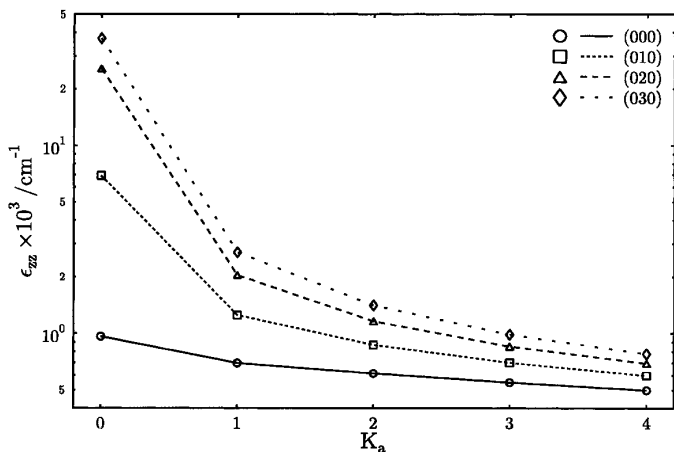


FIG. 3. Calculated values of ϵ_{zz} for K_a ranging from 0 to 4 for the lowest vibrational states of $^{12}\text{CH}_2$.

We can roughly estimate the derivative $\partial D / \partial r$ as $-0.124 \text{ cm}^{-1} / \text{\AA}$ from the *ab initio* work by Harrison (24), who reported data points for different molecular configurations. It is consistent in sign with the work by Langhoff and Kern (27) but deviates significantly from the value of $+0.184 \text{ cm}^{-1} / \text{\AA}$ obtained from our optimized parameter values (see Table 1). This is not, however, a contradiction between our model and the *ab initio* results, but rather between the *ab initio* data and the experimental results for the (100) vibrational states of CH₂ and CD₂. It was already pointed out by Sears *et al.* (14) that for the (100) state of CH₂, the analysis of the experimental led to a change in D which was “considerably larger than, and opposite in sign to, that predicted by Langhoff and Kern” (27).

Further, we can compare the theoretical values of D and

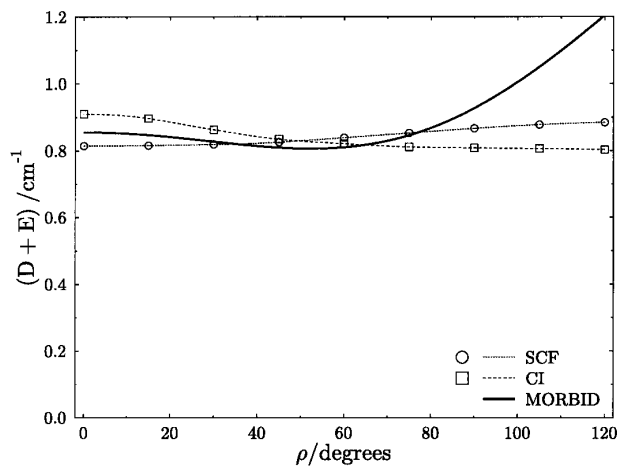


FIG. 4. The parameter $D + E$ plotted against the bending angle ρ . The solid curve shows the results of the present work. Circles and squares represent SCF and CI points, respectively, calculated by Langhoff and Davidson (25).

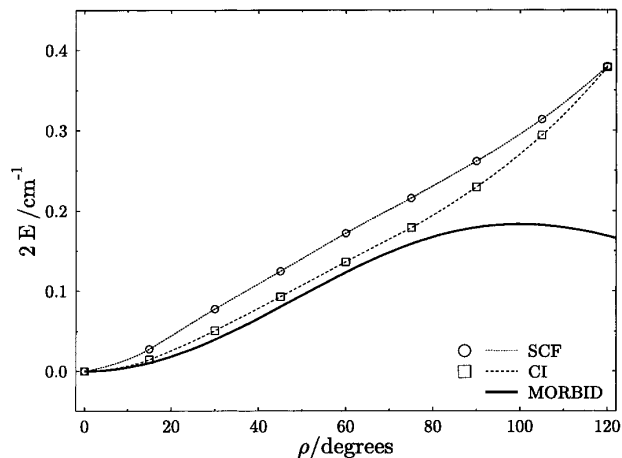


FIG. 5. The parameter $2E$ plotted against the bending angle ρ . The solid curve shows the results of the present work. Circles and squares represent SCF and CI points, respectively, calculated by Langhoff and Davidson (25).

E reported in Ref. (27) for several of the lowest vibrational states of CH₂ with our calculated values presented in Table 3. We conclude that our values deviate stronger from the equilibrium values than do the *ab initio* values, even if we do not consider the K_a dependence. The dependence on K_a was not considered in Ref. (27). However, it is seen from Figs. 1 and 2, which show the D and E values obtained in the present work plotted against K_a for $0 \leq K_a \leq 4$, that also the variation with K_a makes these parameters differ substantially from their equilibrium values. Since we could not determine the stretching dependence of the $(\alpha_{yy} - \alpha_{xx})$ term, the values of E for the (100) and (001) vibrational states are essentially equal to the ground state value and therefore not included in Fig. 2.

Finally our results can be utilized to refine the g tensor for methylene which is used in calculation of Zeeman components particularly for LMR spectroscopy (13). Curl (40) has reported the very useful relation

$$g_{\beta\gamma} = g_e \delta_{\beta\gamma} - \hbar^{-2} \sum \epsilon_{\beta\delta} I_{\delta\gamma} \quad [28]$$

TABLE 3
Spin Interaction Parameters (in cm^{-1}) Calculated for $K_a = 0$ in the Lowest Vibrational States of $^{12}\text{CH}_2$

	(000)	(010)	(020)	(030)	(100)	(001)
$\epsilon_{aa} \times 10^2$	0.096	0.69	2.6	3.7	0.096	0.097
$\epsilon_{bb} \times 10^2$	-0.499	-0.493	-0.495	-0.511	-0.495	-0.502
$\epsilon_{cc} \times 10^2$	-0.430	-0.427	-0.430	-0.439	-0.427	-0.433
$\epsilon_{ba} \times 10^2$	-0.002	-0.002	-0.002	-0.002	-0.003	0.
$\epsilon_{ab} \times 10^2$	0.010	0.013	0.015	0.014	0.020	-0.038
D	0.7788	0.7978	0.8043	0.7986	0.7819	0.7862
$E \times 10$	0.4033	0.3431	0.2937	0.2792	0.4035	0.4037

which couples the \mathbf{g} tensor with the ϵ tensor and the inertial tensor \mathbf{I} . In Eq. [28] $g_e = 2.0023193$ (31). If we take $\mathbf{I}^{-1} \approx \boldsymbol{\mu}$ then it follows straightforwardly from our parameterization of $\epsilon_{\beta\gamma}$ (see Eq. [12]) that

$$g_{\beta\gamma} = g_e \delta_{\beta\gamma} - f_{\beta\gamma}. \quad [29]$$

Since, with the parameters that we can usefully fit (Table 1), our $f_{\beta\gamma}$ values are independent of the molecular geometry, we can calculate that $g_{aa} = 2.0023144(9)$ and $g_{bb} = g_{cc} = 2.002614(4)$.

One intriguing question that has been raised again here is concerned with the comparison between *ab initio* D values and values observed experimentally or calculated with the optimized parameters obtained in the present work. As mentioned above, the *ab initio* results predict $\partial D/\partial r < 0$, whereas experiment requires this derivative to be positive. Further *ab initio* calculations are necessary to investigate whether this discrepancy can be removed by employing larger basis sets in the *ab initio* calculations, or if it is caused by deficiencies inherent in the *ab initio* methods used to calculate D .

ACKNOWLEDGMENTS

We thank P. R. Bunker for encouragement and advice and for critically reading the manuscript. We are grateful to H. M. Pickett for providing us with his program for calculating spin splittings and to E. A. Cohen for help in using this program. This work was supported in part by the Fonds der Chemischen Industrie. I.N.K. is grateful to the German Academic Exchange Service (DAAD) for a fellowship.

REFERENCES

1. P. Jensen, *J. Mol. Spectrosc.* **128**, 478–501 (1988).
2. P. Jensen, *J. Chem. Soc. Faraday Trans. 2* **84**, 1315–1340 (1988).
3. P. Jensen, in "Methods in Computational Molecular Physics" (S. Wilson and G. H. F. Dierksen, Eds.), Plenum Press, New York, 1992.
4. S. Carter and N. C. Handy, *J. Chem. Phys.* **87**, 4294–4301 (1987).
5. S. E. Choi and J. C. Light, *J. Chem. Phys.* **97**, 7031–7054 (1992).
6. M. J. Bramley and T. Carrington, Jr., *J. Chem. Phys.* **99**, 8519–8541 (1993).
7. J. Tennyson, J. R. Henderson, and N. G. Fulton, *Comput. Phys. Commun.* **86**, 175–198 (1995).
8. O. L. Polyansky, P. Jensen, and J. Tennyson, *J. Mol. Spectrosc.* **178**, 184–188 (1996).
9. J. M. Hollis, P. R. Jewell, and F. J. Lovas, *Astrophys. J.* **438**, 259–264 (1995).
10. J. M. Hollis, P. R. Jewell, and F. J. Lovas, *Astrophys. J.* **346**, 794–798 (1989).
11. H. Ozeki and S. Saito, *Astrophys. J.* **451**, L97–L99 (1995).
12. H. Ozeki and S. Saito, *J. Chem. Phys.* **104**, 2167–2171 (1996).
13. T. J. Sears, P. R. Bunker, and A. R. W. McKellar, *J. Chem. Phys.* **75**, 4731–4732 (1981).
14. T. J. Sears, P. R. Bunker, A. R. W. McKellar, K. M. Evenson, D. A. Jennings, and J. M. Brown, *J. Chem. Phys.* **77**, 5348–5362 (1982).
15. T. J. Sears, P. R. Bunker, and A. R. W. McKellar, *J. Chem. Phys.* **77**, 5363–5369 (1982).
16. T. J. Sears, *J. Chem. Phys.* **85**, 3711–3715 (1986).
17. M. D. Marshall and A. R. W. McKellar, *J. Chem. Phys.* **85**, 3716–3723 (1986).
18. F. J. Lovas, R. D. Suenram, and K. M. Evenson, *Astrophys. J.* **267**, L131–L133 (1983).
19. P. R. Bunker, T. J. Sears, A. R. W. McKellar, K. M. Evenson, and F. J. Lovas, *J. Chem. Phys.* **79**, 1211–1219 (1983).
20. K. M. Evenson, T. J. Sears, and A. R. W. McKellar, *J. Opt. Soc. Am. B* **1**, 15–21 (1984).
21. A. R. W. McKellar and T. J. Sears, *Can. J. Phys.* **61**, 480–488 (1983).
22. P. R. Bunker, in "Comparison of Ab Initio Quantum Chemistry with Experiment: State of the Art" (R. J. Bartlett, Ed.), Reidel, Dordrecht, 1985.
23. J. Higuchi, *J. Chem. Phys.* **39**, 1339–1341 (1963).
24. J. F. Harrison, *J. Chem. Phys.* **54**, 5413–5417 (1971).
25. S. R. Langhoff and E. R. Davidson, *Int. J. Quant. Chem.* **7**, 759–777 (1973).
26. S. R. Langhoff, *J. Chem. Phys.* **61**, 3881–3885 (1974).
27. S. R. Langhoff and C. W. Kern, in "Modern Theoretical Chemistry" (H. F. Schaefer III, Ed.), Vol. 4, pp. 381–437, 1977.
28. J. H. Van Vleck, *Rev. Modern Phys.* **23**, 213–227 (1951).
29. W. T. Raynes, *J. Chem. Phys.* **41**, 3020–3032 (1964).
30. R. E. Moss, "Advanced Molecular Quantum Mechanics," Chapman and Hall, London, 1973.
31. I. M. Mills, T. Cvitaš, K. Homann, N. Kallay, and K. Kuchitsu, "Quantities, Units and Symbols in Physical Chemistry," Blackwell Scientific, London, 1993.
32. J. M. Brown and B. J. Howard, *Mol. Phys.* **31**, 1517–1525 (1976).
33. I. C. Bowater, J. M. Brown, and A. Carrington, *Proc. R. Soc. Lond. A* **333**, 265–288 (1973).
34. P. Jensen, *J. Mol. Spectrosc.* **132**, 429–457 (1988).
35. R. N. Zare, "Angular Momentum," Wiley, New York, 1988.
36. P. R. Bunker, "Molecular Symmetry and Spectroscopy," Academic Press, London, 1979.
37. H. M. Pickett, *J. Mol. Spectrosc.* **148**, 371–377 (1991).
38. P. Jensen and P. R. Bunker, *J. Chem. Phys.* **89**, 1327–1332 (1988).
39. J. M. Brown and T. J. Sears, *J. Mol. Spectrosc.* **75**, 111–133 (1979).
40. R. F. Curl, *Mol. Phys.* **9**, 585–597 (1965).